

LOCALIZATION OF NOISE SOURCES IN THE APS STORAGE RING USING THE REAL-TIME FEEDBACK SYSTEM *

Xiang Sun[#] and Glenn Decker, ANL, Argonne, IL 60439, U.S.A.

Abstract

There are two parallel feedback systems to correct the transverse orbit at the Advanced Photon Source (APS) storage ring: a real-time feedback (RTFB) system [1] that runs at 1.5 kHz using 38 fast correctors and up to 160 beam position monitors (BPMs), and a DC feedback system that runs at 10 Hz using up to 317 correctors and over 500 BPMs. An algorithm that uses the open-loop beam motion data to spatially locate strong noise sources in the storage ring is described. The orbit data are measured with 1.5-kHz data acquisition associated with the RTFB system. This system is limited to collecting 40 time-series waveforms synchronously. If synchronous data for the whole ring could be collected, source identification would be straightforward, because a sample-by-sample orbit could be reconstructed with the inverse response matrix. Since this is not the case, a synchronization procedure was developed allowing the splicing together of spatially overlapping double-sector single-frequency trajectories. This technique is applicable to narrow-band noise sources. By multiplying the truncated pseudo-inverse response matrix of the APS storage ring by the synchronous orbit data at a fixed frequency, noise sources at a fixed frequency can be located. The experiment and calculation results are presented.

INTRODUCTION

The real-time orbit feedback system is implemented digitally using digital signal processors (DSPs) [2,3] and consists of 21 VME crates – 1 master and 20 slaves. The 20 slave VME crates are distributed around the circumference of the 40-sector APS storage ring to manage interfaces to BPMs and correctors, and to compute orbit corrections. The master crate provides global controls to the other 20 slave crates and provides analysis tools such as “DSP scope,” which works like a digital oscilloscope. The DSP scope can collect 40 channels synchronously, and each waveform has up to 4080 data points with 1.5 kHz sample rate.

While beam stability at the APS is quite good, there are a significant number of narrow-band spectral lines resulting in elevated levels of beam motion [4,5]. The problem comes from some potential spatially discrete, relatively strong sources of noise.

If one considers a full response matrix mapping all possible sources to all BPMs, a time series approximating each of these noise sources can be estimated by pseudo-inverting the full matrix and multiplying the orbit data that is collected synchronously.

The method for localizing narrow-band noise sources is described below. As a test case, a fast corrector in APS sector 10 was driven with a sine wave at 18.049 Hz. Because DSP scope collects only 40 waveforms at a time, it is not possible to collect data for the entire ring simultaneously. However, a synchronization procedure has been developed that results in a fixed-frequency orbit for the whole ring. After multiplying by the pseudo-inverse response matrix, the location of the known noise source can be reconstructed. This procedure was carried out driving both horizontally and vertically. Having validated the method, the same procedure was applied to a number of examples of unknown narrow-band noise sources.

EXPERIMENT AND CALCULATION TO LOCALIZE NOISE SOURCES

Measurement of the Orbit Changes

We measured the AC orbit by using as many BPMs as possible with the DSP scope tool's double-sector BPM acquisition function with the RTFB loop open. The double-sector BPM acquisition function synchronously collects 40 BPM waveforms at 1.5 kHz. This allows waveforms from ten BPMs per sector horizontally and vertically for two sectors to be acquired. Two such data sets with an overlapping sector can be synchronized with each other by making use of a common spectral line as a type of clock, provided that the spectral line is reasonably stable. By collecting 40 overlapping double-sector data sets in this fashion, one can reconstruct two complete orbits for the 40-sector ring.

We drove the fast correctors S10A:H3 and S10A:V3 separately with a sine wave at 18.049 Hz as a known strong source. The corresponding orbit changes were inferred from 1.5-kHz DSP scope data for 375 different BPMs. This test case was used to validate our method of narrow-band source localization. After stopping the 18.049-Hz excitation, we measured the ambient orbit motion with DSP scope at a 153-Hz sample rate to localize potential narrow-band noise sources in a lower frequency band. All of these measurements were conducted open loop: neither AC nor DC orbit correction systems were active.

*Work supported by U.S. Department of Energy, Office of Science, Office of Basic Energy Sciences, under Contract No. DE-AC02-06CH11357

[#]xiang@aps.anl.gov

The Overlapping Double-Sector AC Orbit Phase Correction Technique

For each of the 20 BPMs (ten per sector) in each data set (horizontal and vertical), the real and imaginary parts of the FFT at the single frequency of interest were extracted, producing a real and imaginary two-sector trajectory at that frequency. A phase rotation was then introduced in such a fashion as to maximize the rms real trajectory while at the same time minimizing the rms imaginary trajectory. If this same phase rotation technique is applied to two double-sector data sets, one finds that the real trajectory in the sector that overlaps is in agreement between the two data sets, outside of an overall sign. By bootstrapping from one double sector (say n and $n+1$) to the next ($n+1$ and $n+2$), while carefully keeping track of sign changes, it is possible to reconstruct a complete AC orbit at a single frequency.

Synchronization

After the orbit data were collected with DSP scope for the whole ring, a fixed-frequency AC orbit for a spectral line of interest was extracted using the technique just described.

Because there are 40 sets of double-sector BPM data for the whole ring, we can generate two independent orbits at a fixed frequency. A comparison between the resulting two orbits, labeled val1 and val2, along with their average, is shown in Figures 1 and 2 for the case of 2-Ampere peak 18.049-Hz oscillations being applied to correctors S10A:H3 and S10A:V3, respectively.

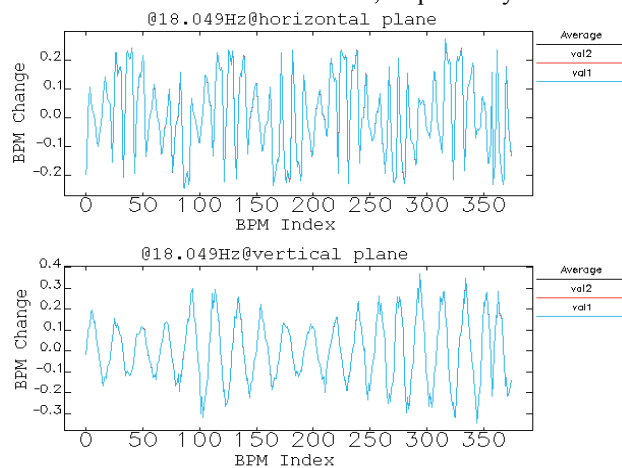


Figure 1: Two groups of synchronous orbit data and their average at 18.049 Hz for both horizontal (top) and vertical (bottom) planes, while driving the beam with a sinusoidal excitation in sector 10.

The two groups of synchronous orbit data (val1 and val2) in Figure 1 agree almost exactly. This indicates that the overlapping narrow-band double-sector phase correction technique is valid for sufficiently strong and stable narrow-band excitation. For the remainder of the analysis, the average of val1 and val2 is used as the best estimate for the AC orbit.

Feedback and instabilities

Shown in Figure 2 is a plot of a column of the response matrix for the corresponding steering corrector in sector 10 (labeled S10A:H3 or S109A:V3), together with the average AC orbit data from Fig. 1 (labeled CalAvg). The response matrix column represents the expected orbit using a corrected ring lattice model. Note that the beam position monitor calibrations are determined from the same algorithm used for the ring lattice corrections, and have been implemented in what follows. [6].

The agreement between measured and theoretical orbits in Fig. 2 is quite good, and in fact, the overlap algorithm used to produce Fig. 1 is a good way to very accurately determine the response matrix empirically.

Shown in Fig. 3 are narrow-band orbit data for two spectral lines observed without external excitation, at 2 Hz horizontally, and 59.98 Hz vertically. The two groups of data in Figure 3 agree well, but show noticeable differences between the two versions of the orbit (val1 vs. val2) in some sectors. This provides a measure of the stability of the measurements during the time required to collect data for the whole ring. Note that the size of these perturbations is two orders of magnitude lower than for the artificially driven results shown in Fig. 1.

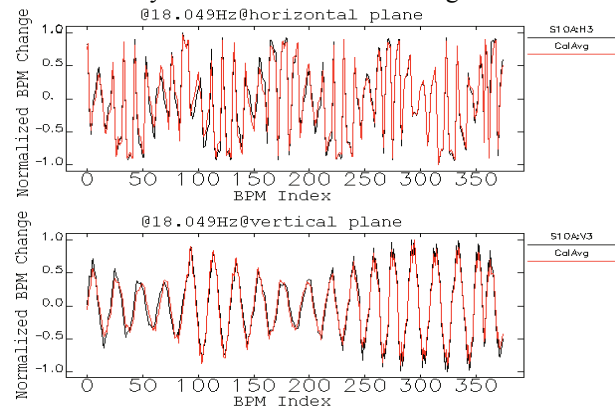


Figure 2: Expected orbit (a column of the response matrix) resulting from driving correctors S10A:H3 (top) and S10A:V3 (bottom). Data with legend CalAvg correspond to the measured average values from Fig. 1 after folding in small calibration corrections.

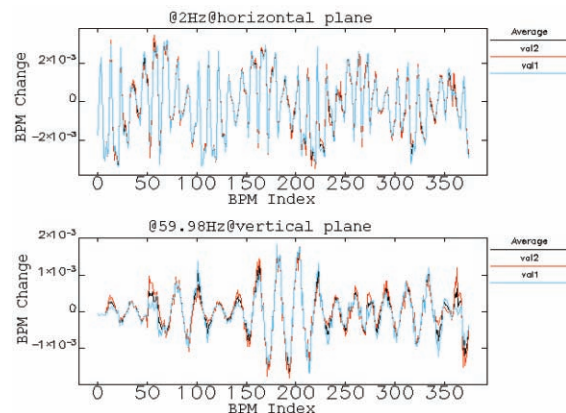


Figure 3: Two groups of synchronous orbit data and their average at 2 Hz in the horizontal plane (top) and at 59.98 Hz in the vertical plane (bottom) without artificial source.

Response Matrix

At APS, there are 375 rf BPMs out of a possible 403 available for monitoring by the real-time feedback system. While there are 317 steering correctors installed, only 38 of them have enough bandwidth for inclusion in the real-time feedback system. In the situation where a string of correctors are used with no BPMs between them, the full response matrix is singular, with infinite condition number. To address this problem, the matrix omitted correctors so that at least one BPM was located between any two successive correctors. After removing the affected correctors and a number of malfunctioning BPMs, the resulting response matrix used 375 rf BPMs and 307 correctors.

In each plane, the $M \times N$ response matrix maps N corrector changes to M BPM changes. When we measure M BPM waveforms simultaneously, we can get all N sources by multiplying the $N \times M$ pseudo-inverse matrix into the M -dimensional array of BPM data as shown in equation (1):

$$\Delta c = R_{pinv}^+ \cdot \Delta b, \quad (1)$$

where Δb is the array of synchronous BPM changes, Δc is the array of sources, and R_{pinv}^+ is the truncated pseudo-inverse response matrix (see equation (3) below.)

SVD and Truncated Pseudo-invert Response Matrix

The response matrix of APS is analyzed by SVD [7] using equation (2)

$$R = U \cdot S \cdot V^T \quad (2)$$

where U and V are orthonormal matrices comprising the eigenvectors, and S is the diagonal matrix of singular values.

Very small singular values lead to large errors after multiplying the pseudo-inverse response matrix with the measured AC orbit, and consequently will result in an acceptable uncertainty for source localization. To deal with this, we zero very small singular values and truncate the pseudo-inverse response matrix as indicated in equation (3):

$$R_{pinv}^+ = V \cdot S_{truncated}^{-1} \cdot U^T, \quad (3)$$

where U and V are the same matrices used in equation (2) and $S_{truncated}^{-1}$ is the inverse of the singular values matrix after the elimination of very small singular values.

If too many singular values are retained, unphysical effects such as noise-induced random step changes from one BPM to the next will result in very large corrector values. On the other hand, if too few singular values are retained, the corrector pattern will be spread over many sectors.

To demonstrate this, we vary the number of singular values for the AC orbit driven by a sine wave at 18.049

Hz on corrector S10A:V3 shown in the lower panel of Fig. 1. The localization results are shown in Figures 4 through 6, using 10, 80, and 150 singular values, respectively. It appears that retaining about 80 singular values is sufficient to localize the noise source for this test case.

Using the same procedure outlined above for the case of the driven 18.049-Hz horizontal orbit shown in the upper panel of Fig. 1, we get the predicted corrector strengths shown in Fig. 7. The peak value in this case corresponds to corrector S10A:H2, which is incorrect, but within one meter of the corrector that was actually causing the disturbance, S10A:H3.

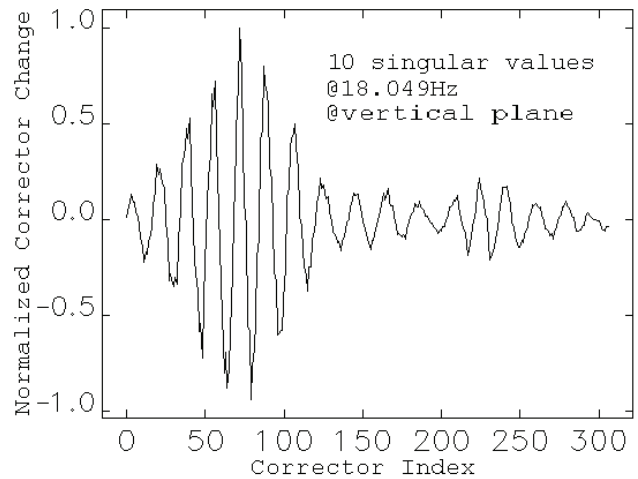


Figure 4: Predicted corrector values resulting from the multiplication of the pseudo-inverse matrix retaining only ten singular values [equation (3)] by the 18.049-Hz vertical orbit shown in the lower panel of Fig. 1.

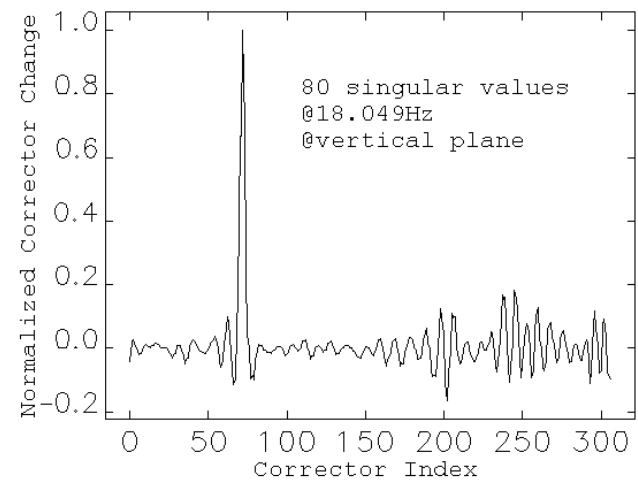


Figure 5: Predicted corrector values, generated in the same fashion as for Fig. 4, but retaining 80 singular values. The peak corresponds to corrector S10A:V3.

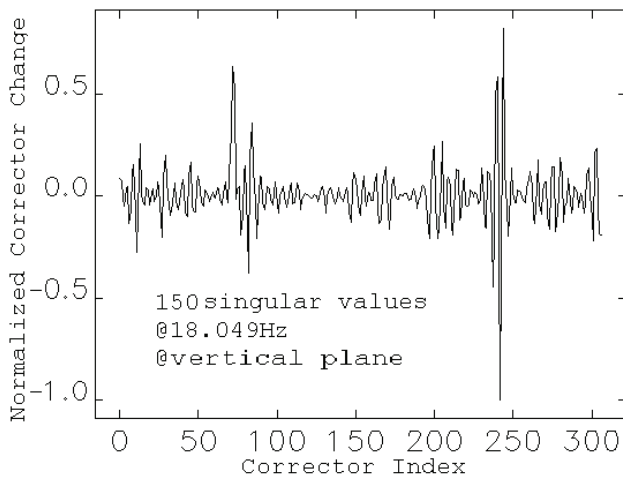


Figure 6: Predicted corrector values, generated in the same fashion as for Figs 4 and 5, but retaining 150 singular values.

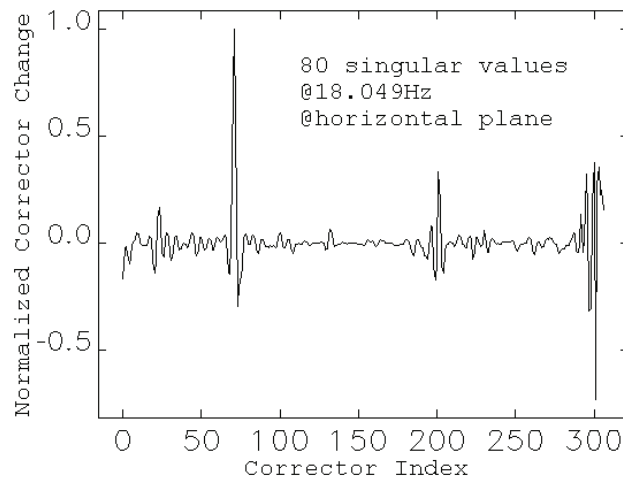


Figure 7: Predicted pattern of correctors derived from the 18.049-Hz horizontal orbit of Fig. 1, caused by deliberately driving corrector S10A:H3. A total of 80 singular values were retained.

Localization of the Unknown Noise Sources

The truncated pseudo-inverse response matrix using synchronous DSP scope BPM data can be used to localize artificial noise sources accurately. In this section we will apply the method to a couple of actual unknown narrow-band noise sources that caused the AC orbits shown in Fig. 3.

We measured the orbit by using the DSP scope tool's double-sector BPM acquisition function with a 154-Hz sample rate. By analyzing the spectra, we noticed spikes at 2-Hz in the horizontal plane and at 59.98-Hz vertically. By multiplying the horizontal truncated pseudo-inverse response matrix by the 2-Hz orbit, we localized the noise source to corrector S38B:H3, shown in Figure 8. With the same process, we localized the noise source at 59.98 Hz to the corrector S1A:V2 in the vertical plane, shown in Figure 9.

Note that for the 2-Hz horizontal case, a large number of singular values were retained in addition to the fact that

there were repeatability problems in the derived AC orbit in this part of the ring. This is apparent by inspecting the upper panel of Fig. 3. These observations, coupled with the knowledge that only three out of a total of ten possible BPMs are available in sector 38, suggest that caution be applied before accepting the apparent noise source indicated by Fig. 8 as being genuine.

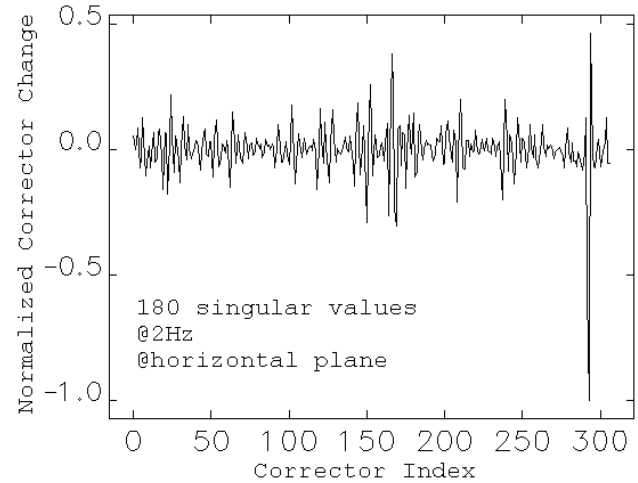


Figure 8: Predicted pattern of correctors corresponding to 2-Hz horizontal orbit of Fig. 3. The peak is located at corrector S38B:H3. Here, 180 singular values are retained.

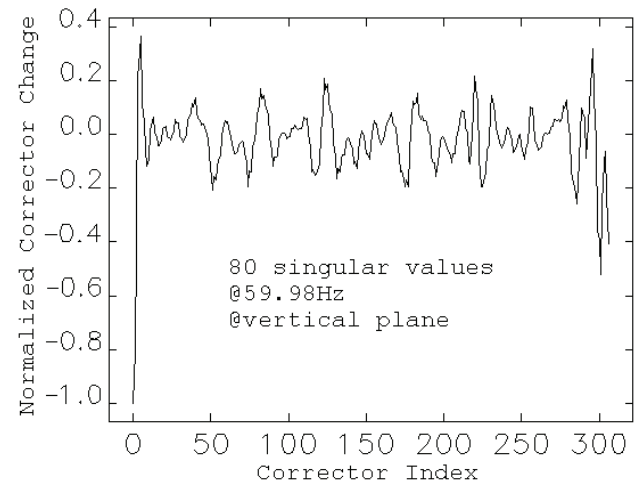


Figure 9: 59.98-Hz noise source in the vertical plane is most likely located at S1A:V2. The first 80 singular values in the ideal vertical response matrix are kept.

CONCLUSION

A technique for extracting AC orbits from 40 non-concurrent time-series data sets with each set comprising 40 waveforms has been developed for narrow-band noise sources. A judicious choice of correctors and singular values allows for the localization of these noise sources at the 1- to 2-meter level. The method has been applied successfully to externally driven AC sources at 18.049

Hz, and preliminary predictions for the locations of real-world ambient noise sources have been made. Further work remains to actually locate the components responsible for these narrow-band excitations and eliminate them.

ACKNOWLEDGEMENTS

The authors wish to acknowledge the contributions of V. Sajaev, H. Shang, L. Emery, and F. Lenkszus upon whose work much of the material presented is based.

REFERENCES

- [1] J. Carwardine and F. Lenkszus, Real-Time Orbit Feedback at the APS, Proceedings of the 1998 Beam Instrumentation Workshop, Palo Alto, CA, AIP Conf Proc. 451, p. 125 (1998).
- [2] J. Carwardine, G. Decker, K. Evans Jr., A. Hillman, F. Lenkszus, R. Merl and A. Pietryla, "Commissioning of the APS Real-time Orbit Feedback System," Proceedings of the 1997 Particle Accelerator Conference, Vancouver, B.C., Canada, <http://www.JACoW.org>, p. 2281 (1998)
- [3] F. Lenkszus, "State-of-the-art Developments in Accelerator Controls at the APS," Proceedings of the 1999 Particle Accelerator Conference, New York, p.333 (1999); <http://JACoW.org>.
- [4] G. Decker, J. Carwardine and O. Singh, "Fundamental Limits on Beam Stability at the Advanced Photon Source," Proceedings of the 1998 Beam Instrumentation Workshop, Palo Alto, CA, AIP Conf. Proc. 451, p. 237 (1998)
- [5] Om Singh and Glenn Decker, "Beam Stability at the Advanced Photon Source," Proceedings of the 2005 Particle Accelerator Conference, Knoxville, Tennessee, p. 3268 (2005) <http://www.JACoW.org>.
- [6] V. Sajaev and L. Emery, "Determination and Correction of the Linear Lattice of the APS Storage Ring," Proc. of EPAC'02, Paris, p. 742 (2002); <http://www.JACoW.org>.
- [7] W. Press, S. Teukolsky, W. Vetterling and B. Flannery, *Numerical Recipes in C 2nd ed.*, Cambridge University Press, New York, 1992.